

Production of Graphene Sheets by Direct Dispersion with Aromatic Healing Agents**

Ming Zhang, Rishi R. Parajuli, Daniel Mastrogiovanni, Boya Dai, Phil Lo, William Cheung, Roman Brukh, Pui Lam Chiu, Tao Zhou, Zhongfan Liu, Eric Garfunkel, and Huixin He*

Graphene exhibits remarkable properties for various novel applications. One of many appealing applications of graphene would be to fabricate transparent conductive films to replace indium tin oxide (ITO). The use of graphene is promising due to its high optical transmittance, low resistance, high chemical stability, and high mechanical strength.^[1] This, as well as other applications, requires a large quantity of high-quality graphene as the basic component.^[2] Among the reported methods to prepare graphene, liquid-phase methods have drawn tremendous attention due to their scalability and ease of functionalization.^[3] Compared to chemical vapor deposition (CVD) approaches, which produce graphene films with the highest conductivity yet obtained,^[4] one advantage of liquid-phase methods is that the produced graphene can be conveniently deposited on any substrate with simple processing, such as spin-coating or inkjet-printing on plastic substrates. Therefore, liquid-based techniques have the potential to realize large-scale organic devices including photovoltaic cells.

Most of the liquid-phase methods involve oxidation of graphite and subsequent exfoliation to form graphene oxide (GO) suspensions. GO is not very conductive, it must be reduced to graphene by toxic hydrazine and/or by annealing at high temperatures in inert conditions to recover much of its electrical conductivity.^[5] Another significant disadvantage of these methods is that the structural defects formed during the oxidation process, which dramatically degrade the unique electronic properties of graphene and its applications, are virtually impossible to repair completely. Recently, Bao and co-workers found that high-temperature annealing is the most effective method to reduce GO to conductive graphene. However, even after annealing at 1100 °C, residual C=O and C–O bonds were still observed by X-ray photoelectron spectroscopy (XPS).^[6a]

Recently, it was reported that graphite can be directly exfoliated in certain solvents to give defect-free mono-layer graphene.^[1b,7] However, these solvents are expensive and require special care when handling. In addition, these solvents tend to have high boiling points, and are difficult to completely remove. Residual solvent results in poor electronic contacts between graphene sheets and therefore lowers the overall conductivity of the resulting multisheet graphene films. Coleman et al. reported a liquid-phase production of graphene by exfoliation of graphite in surfactant/water solutions.^[8] However, the residuals surfactant, similar to solvents with high boiling points, is difficult to remove.

Here, we report a simple and scalable exfoliation approach to produce high-quality single-layer graphene sheets. In a typical experimental procedure, graphite powder was exfoliated by sonicating in an aqueous solution of pyrene molecules that had been functionalized with different water-soluble groups. Highly conductive graphene sheets stabilized in aqueous suspensions were directly produced without requiring toxic reducing agents and expensive solvents. Most importantly, different from other surfactants and polymers that have been used to prevent graphene sheets from aggregation in solution, the pyrene molecules also act as nanographene molecules to heal the possible defects in the graphene sheets during annealing.^[9] Remarkably, they also appear to act as electrical “glue” soldering adjacent graphene sheets, such that electric contacts between graphene sheets can be dramatically improved across the film. Graphene films with a conductivity of

[*] Prof. H. He, M. Zhang, R. R. Parajuli, W. Cheung, Dr. R. Brukh, P. L. Chiu
Chemistry Department, Rutgers University
73 Warren Street, Newark, NJ 07102 (USA)
E-mail: huixinhe@newark.rutgers.edu
D. Mastrogiovanni, Prof. E. Garfunkel
Department of Chemistry and Chemical Biology, Rutgers University
610 Taylor Road, Piscataway, NJ 08854(USA)
B. Dai, Prof. Z. Liu
Center for Nanochemistry
Beijing National Laboratory for Molecular Sciences
State Key Laboratory for Structural Chemistry of Unstable and Stable Species
College of Chemistry and Molecular Engineering, Peking University
Beijing 100871 (P. R. China)
P. Lo, Prof. T. Zhou
Department of Physics
New Jersey Institute of Technology, University Heights
Newark, New Jersey 07102 (USA)

[**] M.Z. and R.R.P. contributed equally to this work. This material is based upon work supported by the National Science Foundation under grant CHE-0750201 and the Rutgers Research Council. H.H. also acknowledges the Trustees Research Fellowship Program at Rutgers, The State University of New Jersey.

DOI: 10.1002/sml.200901978

181200 S m⁻¹ (778 Ω per square) and a light transmittance greater than 90% in the 400–800-nm wavelength range are reproducibly obtained, which is the highest conductivity value ever achieved for graphene films fabricated by graphite-exfoliation approaches (note that graphene films fabricated by the CVD method can reach 200 Ω per square at 80% optical transparency).^[4] Nevertheless, this simple and scalable approach is extremely promising to produce high-quality graphene films for a wide range of optoelectronic applications, including photovoltaics.

Several studies have reported that the excimer emission of pyrene was quenched when GO was reduced in the presence of pyrene molecules functionalized with different water-soluble groups, which has been ascribed to the effective electron or energy transfer between the reduced conductive-graphene and pyrene moiety of the molecules.^[10] Similar quenching phenomena were observed when pyrene derivatives were used to disperse carbon nanotubes, which was explained by energy transfer from the pyrene moieties to the nanotubes. We hypothesize that similar quenching phenomena would occur during direct exfoliation of graphite and therefore we used fluorescence spectroscopy to monitor the exfoliation process.

Figure 1a shows the fluorescence spectra (excited at 340 nm) of a 1-pyrenemethylamine hydrochloride (Py-NH₂)/graphene suspension for different sonication periods. Prior to sonication, the spectrum shows a big peak at 501 nm, which was ascribed to the excimer emission of pyrene derivatives.^[10b,11] We found that the intensity of this peak largely decreased after two hours of sonication. At the same time, we observed a dramatic increase in the peak at 400 nm and a new sharp peak at 385 nm. This fluorescence behavior was virtually the same as that of the Py-NH₂ aqueous solutions alone when the concentration of Py-NH₂ is below its critical micelle concentration, suggesting that the fluorescence of the graphene/Py-NH₂ (Gr-Py-NH₂) solution is derived by the non-bound (free) Py-NH₂ monomers in the solution. The obtained solution was deep grey and stable for two days without any observable aggregation and precipitation. To remove the free Py-NH₂ molecules, the solution was extensively dialyzed against deionized (DI) water (25 times) until the monomer fluorescent peak was almost non-observable. After this extensive dialysis, the solution becomes less stable. A small amount of aggregation and precipitation can be seen after twelve hours.

A similar trend was observed when exfoliation of graphite was performed by sonication in the presence of 1,3,6,8-pyrenetetrasulfonic acid (Py-SO₃) (Figure 1b). In comparison to the case of Py-NH₂ the use of Py-SO₃ resulted in a shorter period of sonication to diminish the excimer peak at 501 nm. Additionally, fewer dialysis cycles were needed to remove sulfonated monomer. We think that these subtle differences may be due to the different solubility of the two pyrene molecules.

It was reported that functionalized pyrene molecules easily form micellar architectures of aggregates due to their amphiphilic nature. The critical micelle concentration of pyrene molecules is as low as 10⁻⁷ M, which may change depending on the functional groups of the pyrene rings.^[11] The intrinsic fluorescence of pyrene derivatives above its critical micellar concentration was ascribed to its excimer emission.^[12]

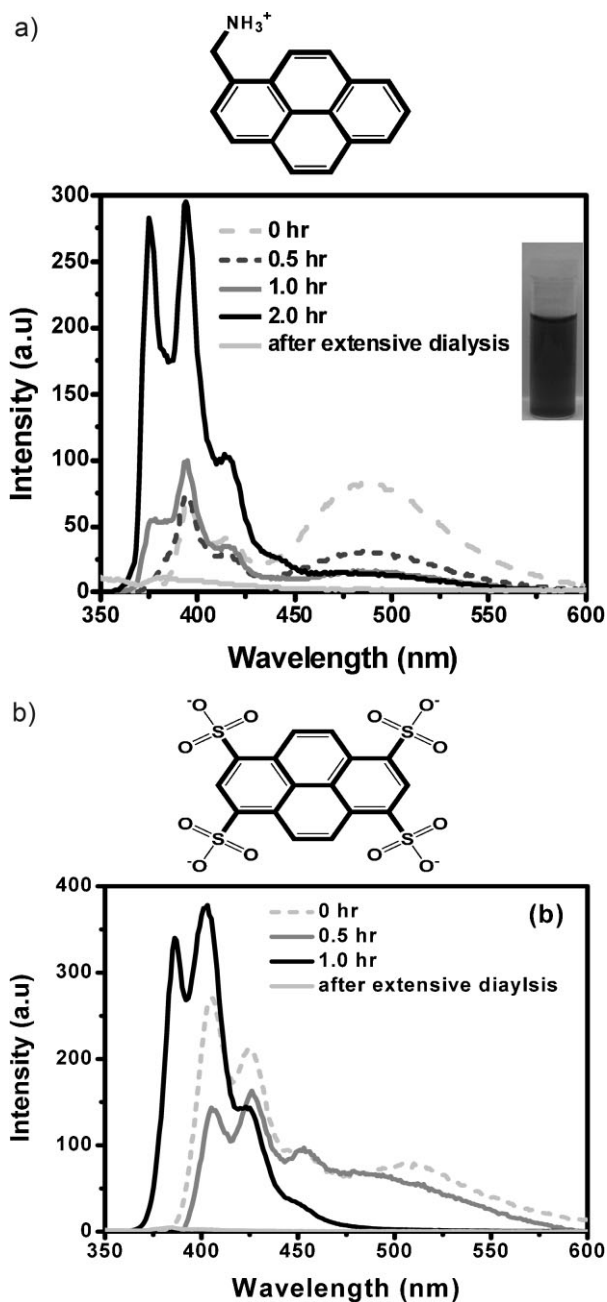
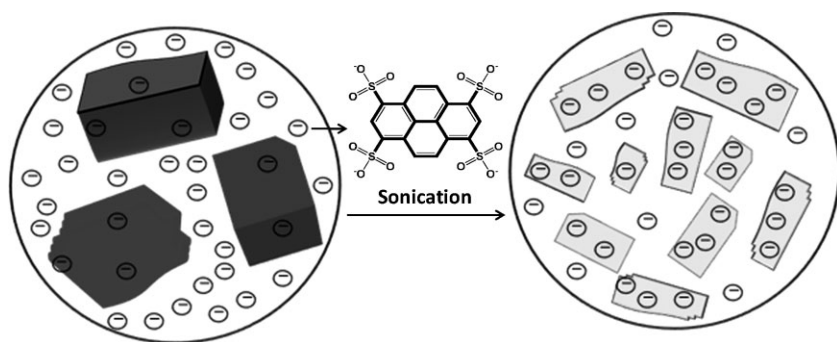


Figure 1. Fluorescence spectroscopy to monitor the direct exfoliation process in the presence of (a) Py-NH₂ and (b) Py-SO₃. Inset: a picture of the resulting graphene suspension.

With sonication, the excimer emission gradually disappeared and was replaced with its monomer emission, indicating that some pyrene molecules adsorbed onto the graphene surface and the equilibrium in the solution phase shifted towards the monomers of pyrene (Scheme 1). The large planar aromatic structures of pyrene molecules can strongly anchor themselves onto the hydrophobic surface of graphene sheets via π - π interactions and yield stable solutions of graphene/pyrene hybrids.^[10b,13] The negative and positive charges in both dispersion molecules act as stabilizing species to maintain a strong static repulsion force between the charged graphene sheets in solution, similar to the scenario when single-walled



Scheme 1. The schematic drawing shows that graphite was exfoliated to graphene sheets with sonication, which dramatically increased the surface area for pyrene-molecule adsorption (here using py-SO₃ as an example). Therefore the concentration of free pyrene molecules in the solution was dramatically decreased; consequently, the excimer emission gradually disappeared and was replaced with its monomer emission of py-SO₃.

carbon nanotubes (SWNTs) were dispersed by 1-(trimethylammonium acetyl) pyrene.^[11]

We used atomic force microscopy (AFM) to characterize the obtained graphene sheets. Figure 2A shows a typical tapping-mode AFM image of Gr-Py-NH₂ hybrids deposited on a freshly cleaved mica surface. The size of the graphene patches are in the micrometer range. The thickness of a single-layer Gr-Py-NH₂ ranges from 0.7 to 1.1 nm with an average of 0.9 ± 0.3 nm, measured from cross-sectional images, as shown in Figure 2C. The variation of thickness was attributed to the possible inhomogeneous coverage of Py-NH₂ molecules on the graphene surface or simply due to the AFM system noises.^[14] Figure 2B shows a typical picture of graphene/Py-SO₃ hybrids (Gr-Py-SO₃). Compared to the Gr-Py-NH₂ sheets, there are some holes with diameters ranging from 20 nm to 500 nm randomly arranged on the Gr-Py-SO₃ graphene sheets. Single-layer graphene shows an average thickness of 1.3 nm

(Figure 2D). Besides the large quantities of single-layer, double-layer graphene with a thickness of 2.6 nm was also observed on the surface, corresponding to the tandem sandwich structures of Gr-Py-SO₃. It was reported that the interlayer distance between pyrene molecules and graphene sheets is 0.35 nm in the graphene hybrid prepared by reduction of GO in the presence of pyrene-1-sulfonic acid, and the pyrene molecules are mainly arranged face-on on both sides of the graphene sheet in a sandwich-like manner.^[10b,13] It is not known yet how Py-SO₃ and Py-NH₂ are arranged on the graphene sheets in the Gr-Py-SO₃ and Gr-Py-NH₂ hybrids prepared here, and further studies are required. The slight difference in the thickness of single-layer Gr-Py-SO₃ and Gr-Py-NH₂ may indicate that the density and the arrangement of Py-SO₃ and Py-NH₂ on the graphene sheets were different. It has been reported that a thickness of more than 1 nm for single-layer graphene sheets by reduction of GO are often observed, which is much larger than the theoretical value of 0.34 nm. This difference has been attributed to some unreduced surface oxygen-containing functional groups.^[15] Therefore, it is also possible that the graphene sheets in these two hybrids consisted of different amounts of oxygen-containing functional groups. Nevertheless, the thicknesses for both of the graphene-pyrene hybrids are smaller than the hybrids prepared by reduction of GO in the presence of pyrene derivatives (1.7 nm).^[10b,13] This deviation in thickness may indicate that fewer oxygen-containing functional groups, therefore fewer defects, were introduced by our simple approach reported here. UV-vis-NIR spectroscopy, X-ray photoelectron spectroscopy, and Raman spectroscopy were used to characterize the hybrids.

UV-vis-NIR spectroscopy measurements of the obtained hybrid suspensions demonstrated that graphene sheets were directly produced without the toxic chemical reduction procedure. It is known that the GO solutions, prepared by the commonly used Hummer and modified Hummer methods,^[16] shows two main features in their UV-vis spectra: i) a peak at 233 nm, which corresponds to a π-π* transition of C=C bond, and ii) a shoulder at ~290–300 nm, corresponding to a π-π* transition of the C=O bond π-π* transition.^[17] Figure 3 shows that after extensive dialysis, the direct exfoliated graphene solutions, both Gr-Py-NH₂ and Gr-Py-SO₃, displayed an absorption maximum at 265 nm with significant tailing in the red region (note that before dialysis of the solution the absorption was dominated by the pyrene derivatives in the UV-vis spectra). The spectra are similar to that of the GO suspension after reduction by NaBH₄ and hydrazine,^[10a] demonstrating again that the π-conjugation of graphene sheets is largely retained during the direct exfoliation process.

XPS was used to characterize the graphene hybrid after deposition from the suspensions onto a gold film (a 100-nm gold layer was sputter-coated on silicon with a 10-nm Ti adhesion layer). The thickness of the graphene hybrids on the gold substrates is roughly 30 nm. The XPS spectra of the two

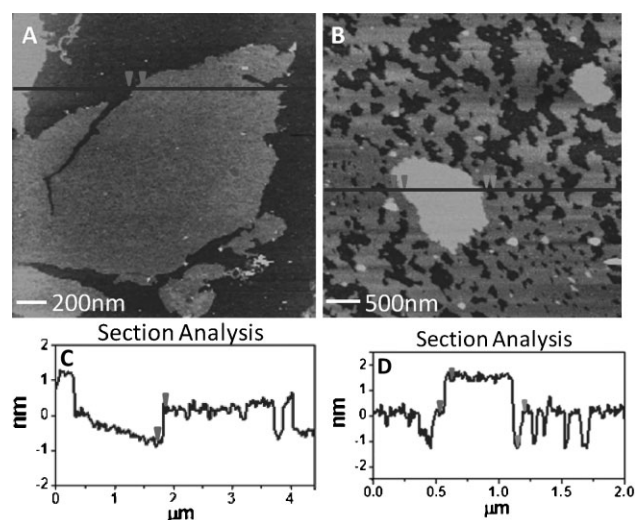


Figure 2. Atomic force microscopy (AFM) images of the graphene sheets on a mica substrate, A) Gr-Py-NH₂ and B) Gr-Py-SO₃. Panels C) and D) are the section analysis of the AFM image in A) and B), respectively, along the black line. The arrows in the pictures help to show the height of the graphene sheet.

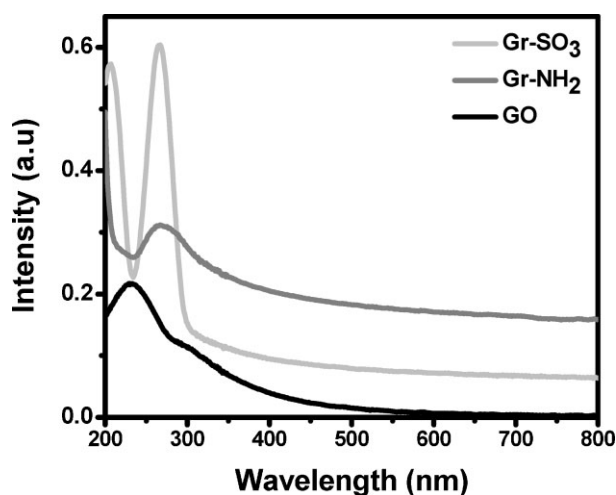


Figure 3. UV-vis spectra of the graphene suspension dispersed by Py-NH₂ and Py-SO₃. For comparison, the UV-vis spectrum of graphite oxide suspension, prepared by the traditional Hummer method is also shown.

hybrids are shown in Figure 4. The C1s signal consisted of four different peaks: C=C/C-C in aromatic rings (284.6 eV), C-O (286.1 eV), C=O (287.5 eV), and C(=O)-OH (289.2 eV) consistent with literature assignments.^[6b] If a homogenous distribution of carbon and oxygen throughout the bulk of the sample is assumed, the C/O ratio for Gr-Py-NH₂ is ~10.7 and for Gr-Py-SO₃ is ~5.3 (after excluding the oxygen contribution from the SO₃ groups). This represents ~4 times and approximately twice the C/O ratio (~2.5) associated with the pristine GO produced by Hummer's method.^[18] The sp² C-C component in the as-produced Gr-Py-NH₂ and Gr-Py-SO₃ hybrids is 76% and 62%, (sp² C/total C + O), respectively. The total oxygen component in the as-produced Gr-Py-NH₂ and Gr-Py-SO₃ hybrids is 8.5% and 16%, respectively. This calculation demonstrates that less defects exist in the Gr-Py-NH₂ films than in those produced with Gr-Py-SO₃ hybrids, consistent with the AFM study described above. Note that the sp² C-C and oxygen components in both as-produced hybrids are very close to the maximum carbon sp² (80%) and minimum oxygen fraction (8%) of reduced GO upon annealing at 1100 °C,^[18] further confirming that we can produce high-quality graphene sheets with less oxidation.

Raman spectroscopy was used to characterize the obtained hybrid suspensions after deposition onto a Si substrate with a 300-nm-thick SiO₂ layer. The typical features of the G band at 1585 cm⁻¹ and the D band at 1335 cm⁻¹ are shown in the Raman spectra (Fig. 5), which agrees well with the literatures by direct exfoliation approaches.^[7a,7c,8] The G band is usually assigned to the E_{2g} phonon of C sp² atoms, while the D band is a breathing mode of κ-point phonons of A_{1g} symmetry. The A_{1g} mode is attributed to particle-size effects due to the existence of specific vibrations at the edges of graphene sheets. The appearance of a prominent D band in the spectrum is also an indication of disorder in graphene originating from the defects associated with vacancies and grain boundaries.^[19] It has been well documented that the size of the defect-free sp² cluster regions is the inverse of the ratio of the D and the G band integrated

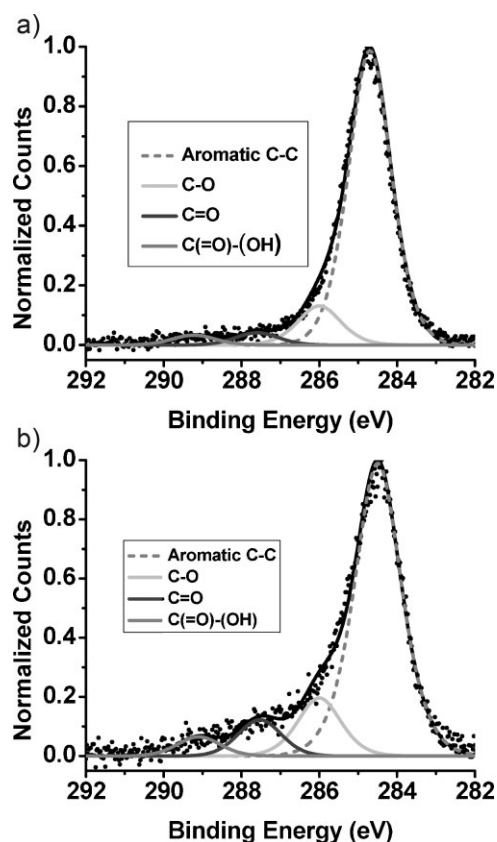


Figure 4. C1s XPS spectra collected on 30 nm as produced graphene hybrids deposited on gold substrates: a) a Gr-Py-NH₂ film and b) a Gr-Py-SO₃ film. The spectra were fitted by a Doniach-Sunjić function after the subtraction of the Shirley background.

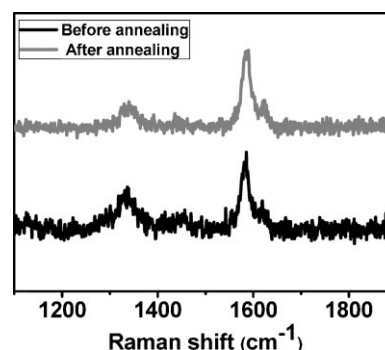


Figure 5. Raman spectra of Gr-Py-SO₃ deposited on Si substrate with a 300-nm layer of SiO₂.

intensities (I_D/I_G).^[20] This correlation has been used to determine the size of sp² domains in various carbon materials including graphene.^[19b,20] After baseline correction, I_D/I_G of the hybrid suspensions was calculated to be 0.64, which is much lower than those graphene sheets obtained from reduction of GO by hydrazine ($I_D/I_G \approx 1.44$)^[21] and the recently reported sodium hydride reduction process ($I_D/I_G \approx 1.08$).^[22] It is even smaller than that achieved by the supercritical-water-based reduction process ($I_D/I_G \approx 0.9$)^[23] and the 180 °C solvothermal reduction process ($I_D/I_G \approx 0.9$).^[24] Therefore, similar to the

other reported direct exfoliation approaches,^[1b,7–8] the simple exfoliation approach provided in this work can also produce graphene sheets with much less defects.

Using the empirical Tuinstra–Koenig relation,^[19b] we found that the size of the ordered crystallite graphitic domain was ≈ 7.0 nm in the as-produced Gr-Py-SO₃. It has been demonstrated that large sp²-domain sizes that are minimally interrupted by defects are essential for obtaining exceptionally high conductivity and mobility in reduced GO. The large domain sizes in the as-produced graphene hybrids further demonstrate the high quality of the graphene sheets dispersed by this simple method. Furthermore, after annealing at 1000 °C for 6 min, the ratio of I_D/I_G further decreased to 0.46, corresponding to an increase in the sp²-domain size to ≈ 9.6 nm. This suggests that the annealing of the hybrid films can further recover the aromatic structures by repairing defects. This observation is very different from the recent reports by Chhowalla and co-workers, who systematically studied deoxidation and structural evolution of GO during thermal annealing by XPS and Raman spectroscopy.^[6b,6c] They found that annealing GO at different temperatures, even at 1100 °C, did not increase the size of defect-free sp² domains significantly, even though the sp² carbon–carbon bonds were restored by deoxidation. They explained this observation as the generation of vacancies in the lattices and dangling bonds from the detachment of CO groups, especially at high temperatures. However, our result is consistent with the report by Mullen et al.^[13] Pyrene molecules in graphene hybrids can be decomposed under thermal annealing, which induced a thermal reaction between pyrene and graphene sheets and resulted in a better π -conjugation of the graphene basal plane. Therefore, larger defect-free sp² domains were produced and the conductivity of graphene films was increased dramatically.

We prepared graphene films from the obtained suspensions with different thickness by a vacuum filtration method through an anodisc filter membrane.^[5a,25] To understand if the performance of the graphene film can replace ITO in solar cells and other optoelectronic applications, we studied the electrical properties of the graphene sheets by measuring the sheet resistance of the corresponding graphene films with a four-probe approach. To study the optical properties, these films were transferred from the anodisc filter membranes onto polydimethylsiloxane (PDMS) sheets and the sheet transmittance was measured in the wavelength range of 400–800 nm. The reported transmittance here was corrected by subtracting the absorption of the same thickness PDMS sheet at each wavelength from the measured absorption curves. As expected, the graphene films show a percolation electronic behavior. The sheet resistance and the transmittance of the graphene film decrease with increasing the amounts of graphene used to prepare the films, as shown in Figure 6. Gr-Py-NH₂ films reach percolation slightly earlier than the Gr-Py-SO₃ films. After reaching the percolation threshold, the sheet resistance of the Gr-Py-NH₂ films is 1.3 k Ω per square at a transmittance of 41 %, and the sheet resistance of the Gr-Py-SO₃ films is 1.1 k Ω per square at a transmittance of 40%. These correspond to a DC conductivity of 1900 S m⁻¹ and 2150 S m⁻¹ for Gr-Py-NH₂ and Gr-Py-SO₃, respectively (the thickness of the film was estimated according to the reports by Bao and co-workers^[6a]

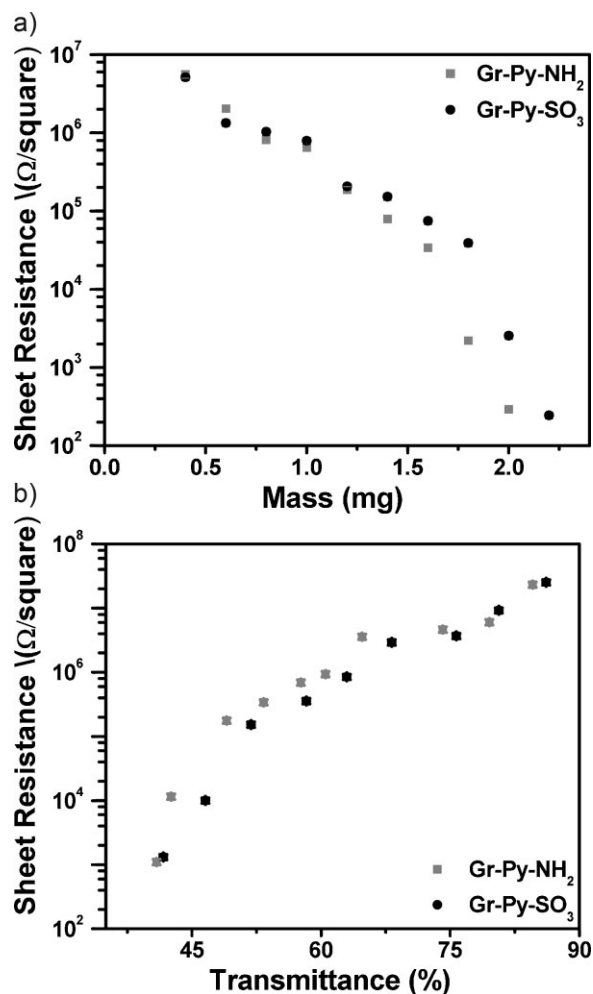


Figure 6. a) Sheet resistance of the graphene films as a function of the weight of the graphene sheet in solution to prepare the graphene films. b) Sheet resistance of the graphene films as a function of the transmittance of the corresponding films.

and Mullen and co-workers^[26]). Even though these values are slightly better than that of sodium dodecylbenzene sulfonate (SDBS) directly exfoliated graphene films reported by Coleman and co-workers^[8] (35 S m⁻¹ before annealing), they are still much lower than the films prepared from *N*-methylpyrrolidone-based dispersions^[7a] (6500 S m⁻¹). We believe the low conductivity was due to the presence of residual pyrene molecules on graphene sheets. Similar to the case of SDBS, the nonconductive pyrene molecules largely impede the electrical contact between graphene sheets in the film, which results in the low conductivity of the films.

However, different from SDBS,^[8] which is difficult to be removed completely, the pyrene molecules here can serve as nanographene building blocks to heal defects in the graphene film during a thermal annealing process.^[13] Therefore, we expect that graphene films with high transparency and high conductivity can be fabricated, which can be used as an ITO replacement material for solar cells and other electroptical applications. To make a transparent and highly conductive film, we prepared films on quartz by drop-coating with a sheet

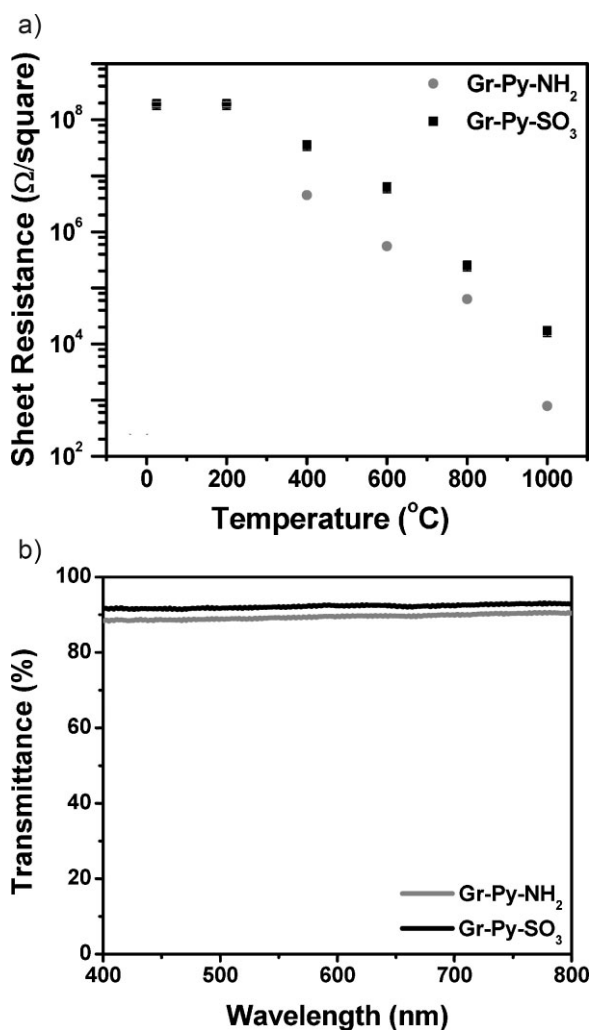


Figure 7. a) The sheet resistance of thin graphene films prepared on quartz substrates by drop coating as function of the annealing temperatures. The concentration of graphene for both of the hybrid suspensions is roughly 0.1 mg L^{-1} . b) The corresponding optical transmittance of the films.

resistance of $1.9 \times 10^8 \Omega \cdot \text{m}^{-1}$ and a transmittance of 90% between a wavelength range of 400–800 nm. The samples were annealed at different temperatures before being cooled to room temperatures for various measurements. As demonstrated in Figure 7, the thermal annealing at 400°C decreased the sheet resistance to $3.5 \times 10^7 \Omega$ per square and $4.5 \times 10^6 \Omega$ per square for Gr-Py-NH₂ and Gr-Py-SO₃, respectively. At 1000°C , the sheet resistance was further decreased to $1.7 \times 10^4 \Omega$ per square and 778Ω per square at 90% transmittance (within a 400–800 nm wavelength range), which correspond to conductivities of 8400 S m^{-1} and 181200 S m^{-1} for Gr-Py-NH₂ and Gr-Py-SO₃, respectively. Note that the conductivity of the graphene prepared from the graphene suspensions with extensive dialysis did not increase significantly. The purity of Ar is also critical for the successful healing of the graphene, otherwise the films can be quickly lost, likely through reactions with residual oxygen in the system. From studies by AFM, UV-vis-NIR spectroscopy, XPS and Raman spectroscopy, we understand that more

defects existed in Gr-Py-SO₃ films compared to those of Gr-Py-NH₂, so it is a surprise to us that the conductivity of Gr-Py-SO₃ films increased much faster than those of Gr-Py-NH₂ upon annealing. Currently we are studying the annealing mechanism by in situ XPS studies to explain this interesting observation, which will be reported later. Nevertheless, it is worth mentioning that films prepared from reduced GO have displayed conductivities ranging from 7200 S m^{-1} [5c] to 10200 S m^{-1} . [6a] In addition, Mullen and co-workers [13] reported that high-temperature annealing of graphene/pyrene composites (at 1100°C), which were obtained by reduction of GO in the presence of pyrene derivatives, led to graphene films with a conductivity around 110000 S m^{-1} . Therefore, the conductivity of the graphene films combined with the high transparency achieved by our approach reached the highest conductivity values ever achieved for graphene films from liquid exfoliation processes, which make our simple and scalable approach extremely attractive to produce high-quality graphene films.

We believe that the remarkable high performance of the graphene films is due to our unique fabrication method, which dramatically reduced structural defects in individual graphene sheets and also improved the electrical contacts between graphene sheets in the films. First, the direct exfoliation of graphite powder in the presence of pyrene derivatives produced graphene sheets with fewer defects compared to the traditional GO-reduction methods. [1b,7a,8] In addition, the novel reparative thermal annealing of the graphene films, in which the pyrene derivatives acted as healing agents during thermal treatment, further repaired some of the defects. [13] Most importantly, the electrical contacts between graphene sheets in the film are also dramatically improved. The pyrene molecules, which originally adsorbed on both sides of the graphene sheets and electrically “glue” them together during the thermal annealing process.

In summary, we developed a simple and scalable exfoliation approach to produce high-quality single-layer graphene sheets (rather than nonconductive graphene oxide) in one step, which can be used to fabricate transparent conductive films. Compared to the traditional GO approach to produce conductive graphene sheets, there is no oxidation and reduction reaction of GO involved. Toxic and expensive solvents are not needed. Our method decreases the number of preparation steps and significantly shortens the production time. Compared to other direct exfoliation methods, this method does not require high-boiling-point solvents. The lack of residual solvents and other impurities results in much better electrical contacts between graphene sheets, needed to produce highly conductive graphene films. In a typical experimental procedure, graphite powders were exfoliated in a water solution of pyrene derivatives with the help of sonication. The pyrene derivatives acted as dispersion agents during the exfoliation process and also acted as healing agents and electric “glue” during the thermal annealing process. Transparent conductive films fabricated with this approach exhibit a conductivity of 181200 S m^{-1} (sheet resistance of 778Ω per square with 90% light transmittance in the 400–800 nm wavelength range), the best to date of which we are aware. Transparent conductive

graphene films are promising candidates to replace transparent conductive oxides (TCOs) for photovoltaic (PV)/solar cell applications.

Experimental

Materials: Synthetic graphite powder (<20 μm), 1-pyrene-methylamine (Py-NH₂) hydrochloride from Sigma-Aldrich, and 1,3,6,8-pyrenetetrasulfonic acid (Py-SO₃) tetrasodium salt hydrate from Acros Organic were purchased and used as received. All solutions were prepared using deionized water (18.2 M Ω) (Nanopure water, Barnstead), which was also used to rinse and clean the samples.

Dispersion of graphene with pyrene molecules: Stock solutions of Py-NH₂ and Py-SO₃ with a concentration 0.4 mg mL⁻¹ were prepared in deionized water by vigorous stirring for 1 h. Graphite powder was added into the resulted solutions, in which the weight ratio between the pyrene derivatives to the graphite powder is 4:1. Direct exfoliation of graphite to graphene sheets was performed by sonication of the obtained mixture solution with Sonics VX-130 (130W, 45%) in an ice bath. The exfoliation process was monitored by recording the fluorescence spectra of the suspension at different exfoliation period. All fluorescence measurements were performed using a Cary-Eclipse fluorescence spectrophotometer (Varian, Inc, Palo Alto, CA). The obtained grey dispersion was then centrifuged at 4000 rpm for 20 min to remove unexfoliated graphite using a Beckman J2-21 centrifuge (usually a very small amount). The supernatant containing graphene sheets was dialyzed three times with an Amicon YM-50 centrifugal filter unit (Millipore) to remove most of the free pyrene molecules. The removal of free pyrene was monitored by measuring UV-vis and emission spectra of the solution after each dialysis. The yield of graphene sheets was estimated to be 50%. The resulted solution was directly used to prepare graphene films with a vacuum filtration method.

Atomic force microscopy: The Py-NH₂ and Py-SO₃ exfoliated graphene samples (after being extensively dialyzed, normally 25 times for Py-NH₂ and 10 times for Py-SO₃) were imaged with a tapping mode Nanoscope IIIa AFM instrument (Veeco instrument, Santa Barbara, CA, USA) in air. In order to image the graphene sheets, 2 μL of the prepared solutions were deposited on freshly cleaved mica. After a 3–5 min of incubation, the mica surface was rinsed with 1 drops of DI water and dried in a fume hood for 20–30 min. During imaging, a 125- μm -long rectangular silicon cantilever/tip assembly (Model: MPP-12100, Veeco) was used with a resonance frequency of approximately 127–170 kHz, a spring constant of approximately 5 N m⁻¹, and a tip radius of less than 10 nm. The applied frequency was set on the lower side of the resonance frequency and scan rate was \sim 1.0 Hz. Height differences were obtained from section analysis of the topographic images. In the figures variations in height are indicated by color coding.

X-Ray Photoelectron Spectroscopy: XPS spectra were obtained with a Perkin-Elmer hemispherical analyzer with a non-monochromatic Mg K α X-ray source ($h\nu = 253.6$ eV). At 17.9 eV pass energy, the full width at half maximum (FWHM) of the Cu 2p 3/2 core level is 1.2 eV. All core-level photoemission peaks were referenced to the Au 4f 7/2 peak with a binding energy of 83.7 eV.

Raman spectroscopy: Raman spectra were acquired with a micro-Raman spectroscope (Renishaw 1000) assembled with a confocal imaging microscope, with an excitation energy of 1.96 eV (632.8 nm) and a power around 0.1 W \sim 0.3 W. Spectra are acquired using a 30 s exposure time and two accumulations.

Optical and electrical properties of the dispersed graphene sheets: UV-vis-NIR absorption spectroscopy was used to characterize the electronic states of the exfoliated graphene sheets. All spectra were obtained using a Cary 500 UV-vis-NIR spectrophotometer in double-beam mode.

Preparation of graphene films: Graphene films with different thickness were prepared from the corresponding suspension by vacuum filtration using Anodisc 47 inorganic membranes with 200-nm pores (Whatman Ltd.). After filtration, the thin films were dried in air for 15–20 min. The sheet resistance of the films was determined by a 302 manual four-point resistivity probe (Lucas Laboratories). To study the optical properties, these films were transferred from the anodisc filter membranes onto PDMS sheets and the sheet transmittance was measured using a Cary 500 UV-vis-NIR spectrophotometer in double-beam mode in the wavelength range of 400–800 nm. The transmittance reported here was corrected by subtracting the absorption of the same thickness PDMS sheet at each wavelength from the measured absorption curves.

To make a transparent and highly conductive film, graphene films on quartz were prepared by drop coating. The films were annealed at different temperatures with a Lindberg Blue oven in high-purity Ar. Electrical and optical properties of the annealed films were measured after being cooled to room temperatures.

Keywords:

doping agents · graphene · healing agents · reparative thermal annealing · transparent conductive oxides

- [1] a) X. Wang, L. Zhi, K. Mullen, *Nano Lett.* **2008**, *8*, 323; b) P. Blake, P. D. Brimicombe, R. R. Nair, T. J. Booth, D. Jiang, F. Schedin, L. A. Ponomarenko, S. V. Morozov, H. F. Gleeson, E. W. Hill, A. K. Geim, K. S. Novoselov, *Nano Lett.* **2008**, *8*, 1704.
- [2] M. Choucair, P. Thordarson, J. A. Stride, *Nature Nanotechnol.* **2009**, *4*, 30.
- [3] S. Park, R. S. Ruoff, *Nature Nanotechnol.* **2009**, *4*, 217.
- [4] K. S. Kim, Y. Zhao, H. Jang, S. Y. Lee, J. M. Kim, J. H. Ahn, P. Kim, J. Y. Choi, B. H. Hong, *Nature* **2009**, *457*, 706.
- [5] a) G. Eda, G. Fanchini, M. Chhowalla, *Nature Nanotechnol.* **2008**, *3*, 270; b) V. T. Tung, M. J. Allen, Y. Yang, R. B. Kaner, *Nature Nanotechnol.* **2008**; c) D. Li, M. B. Muller, S. Gilje, R. B. Kaner, G. G. Wallace, *Nature Nanotechnol.* **2008**, *3*, 101.
- [6] a) H. A. Becerril, J. Mao, Z. F. Liu, R. M. Stoltenberg, Z. Bao, Y. S. Chen, *ACS Nano* **2008**, *2*, 463; b) C. Mattevi, G. Eda, S. Agnoli, S. Miller, K. A. Mkhoyan, O. Celik, D. Mastrogianni, G. Granozzi, E. Garfunkel, M. Chhowalla, *Adv. Funct. Mater.* **2009**, *19*, 2577; c) K. A. Mkhoyan, A. W. Contryman, J. Silcox, D. A. Stewart, G. Eda, C. Mattevi, S. Miller, M. Chhowalla, *Nano Lett.* **9**, 1058.
- [7] a) Y. Hernandez, V. Nicolosi, M. Lotya, F. M. Blighe, Z. Y. Sun, S. De, I. T. McGovern, B. Holland, M. Byrne, Y. K. Gun'ko, J. J. Boland, P. Niraj, G. Duesberg, S. Krishnamurthy, S. Goodhue, J. Hutchison, V. Scardaci, A. C. Ferrari, J. N. Coleman, *Nature Nanotechnol.* **2008**, *3*, 563; b) A. B. Bourlino, V. Georgakilas, R. Zboril, T. A. Steriotis, A. K. Stubos, *Small* **2009**, *5*, 1841; c) A. B. Bourlino, V. Georgakilas, R. Zboril, T. A. Steriotis, A. K. Stubos, C. Trapalis, *Solid State Commun.* **2009**, *149*, 2172.

- [8] M. Lotya, Y. Hernandez, P. J. King, R. J. Smith, V. Nicolosi, L. S. Karlsson, F. M. Blighe, S. De, Z. Wang, I. T. McGovern, G. S. Duesberg, J. N. Coleman, *J. Am. Chem. Soc.* **2009**, *131*, 3611.
- [9] L. Liu, K. T. Rim, D. Eom, T. F. Heinz, G. W. Flynn, *Nano Lett.* **2008**, *8*, 1872.
- [10] a) Y. Y. Liang, D. Q. Wu, X. L. Feng, K. Mullen, *Adv. Mater.* **2009**, *21*, 1679; b) Y. Xu, H. Bai, G. Lu, G. Q. Shi, *J. Am. Chem. Soc.* **2008**, *130*, 5856.
- [11] C. Ehli, G. M. A. Rahman, N. Jux, D. Balbinot, D. M. Guldi, F. Paolucci, M. Marcaccio, D. Paolucci, M. Melle-Franco, F. Zerbetto, S. Campidelli, M. Prato, *J. Am. Chem. Soc.* **2006**, *128*, 11222.
- [12] F. M. Winnik, *Chem. Rev.* **1993**, *93*, 587.
- [13] Q. Su, S. Pang, V. Alijani, C. Li, X. L. Feng, K. Mullen, *Adv. Mater.* **2009**, *21*, 3191.
- [14] X. C. Dong, Y. M. Shi, Y. Zhao, D. M. Chen, J. Ye, Y. G. Yao, F. Gao, Z. H. Ni, T. Yu, Z. Shen, Y. X. Huang, P. Chen, L. J. Li, *Phys. Rev. Lett.* **2009**, *102*, 135501.
- [15] S. Stankovich, D. A. Dikin, R. D. Piner, K. A. Kohlhaas, K. A. Kleinhammes, Y. Jia, Y. Wu, S. B. Nguyen, R. S. Ruoff, *Carbon* **2007**, *45*, 1558.
- [16] Z. T. Luo, Y. Lu, L. A. Somers, A. T. C. Johnson, *J. Am. Chem. Soc.* **2009**, *131*, 898.
- [17] *UV Spectroscopy: Techniques, Instrumentation, Data Handling*, Vol. 4 (Eds: B. J. Clark, T. Frost, M. A. Russell), Chapman & Hall, New York **1993**.
- [18] C. Hontorialucas, A. J. Lopezpeinado, J. D. D. Lopezgonzalez, M. L. Rojascervantes, R. M. Martinaranda, *Carbon* **1995**, *33*, 1585.
- [19] a) A. C. Ferrari, J. C. Meyer, V. Scardaci, C. Casiraghi, M. Lazzeri, F. Mauri, S. Piscanec, D. Jiang, K. S. Novoselov, S. Roth, A. K. Geim, *Phys. Rev. Lett.* **2006**, *97*; b) F. Tuinstra, J. L. Koenig, *J. Chem. Phys.* **1970**, *53*, 1126.
- [20] L. G. Cancado, K. Takai, T. Enoki, M. Endo, Y. A. Kim, H. Mizusaki, A. Jorio, L. N. Coelho, R. Magalhaes-Paniago, M. A. Pimenta, *Appl. Phys. Lett.* **2006**, *88*.
- [21] V. T. Tung, M. J. Allen, Y. Yang, R. B. Kaner, *Nat. Nanotechnol.* **2009**, *4*, 25.
- [22] N. Mohanty, A. Nagaraja, J. Armesto, V. Berry, *Small* **2010**, *6*, 226.
- [23] Y. Zhou, Q. Bao, L. A. L. Tang, Y. Zhong, K. P. Loh, *Chem. Mater.* **2009**, *21*, 2950.
- [24] H. L. Wang, J. T. Robinson, X. L. Li, H. J. Dai, *J. Am. Chem. Soc.* **2009**, *131*, 9910.
- [25] Z. Wu, Z. Chen, X. Du, J. M. Logan, J. Sippel, M. Nikolou, K. Kamaras, J. R. Reynolds, D. B. Tanner, A. F. Hebard, A. G. Rinzler, *Science* **2004**, *305*, 1273.
- [26] X. Wang, L. Zhi, N. Tsao, Z. Tomovic, J. Lin, K. Mullen, *Angew. Chem. Int. Ed.* **2008**, *47*, 2990.

Received: October 20, 2009

Revised: February 16, 2010

Published online: